J. Innovative Eng. Nat. Sci., vol. 6, no. 1, pp. 242-257, 2026.
http://doi.org/10.61112/jiens.1718642

Original Paper

Journal of Innovative Engineering and Natural Science
(Yenilikçi Mühendislik ve Doğa Bilimleri Dergisi)
https://dergipark.org.tr/en/pub/jiens

Development of gelatin-chitosan composite nanofibers incorporated with Corncob-derived cellulose microcrystals

Salih Birhanu Ahmed[a], Beyza Soydan[b], Cigdem Ucar[b], Emine Tekcan[b], Ali Toptas[c], Harun Cug[a] and Yasin Akgul[d,*]

[a]*Mechanical Engineering Department, Karabuk University, 78050 Karabuk, Türkiye.*
[b]*Biomedical Engineering Department, Karabuk University, 78050 Karabuk, Türkiye.*
[c]*Textile Engineering Department, Istanbul Technical University, 34467 Istanbul, Türkiye.*
[d]*Iron and Steel Institute, Karabuk University, 78050 Karabuk, Türkiye.*

ARTICLE INFO

Article history:
Received June 12, 2025
Received in revised form September 23, 2025
Accepted October 11, 2025

Available online

Keywords:
Cellulose microcrystal
Nanofiber
Gelatin
Chitosan
Sustainable

ABSTRACT

The increasing demand for sustainable, antibacterial, and eco-friendly food packaging materials has intensified research into biodegradable biopolymers with enhanced functional properties. In this study, gelatin–chitosan-based nanofibers were fabricated via electro-blowing and reinforced with cellulose microcrystals (CMC) extracted from corn cobs via acid hydrolysis. The formulation (12% gelatin and 3% chitosan) and electro-blowing parameters were optimized based on previous literature and preliminary trials to ensure uniform fiber morphology. CMC was incorporated at concentrations of 1, 3, and 5% (w/w), and the resulting nanofibers were characterized using FE-SEM, ATR-FTIR, XRD, TGA, and air permeability tests. SEM analysis revealed smooth, bead-free fibers with average diameters ranging from 642.19 ± 40.36 nm (control) to 760.05 ± 32.64 nm (3% CMC), confirming the impact of filler loading. XRD results demonstrated an increase in crystallinity from 21.3% in the control to 27.8% with 5% CMC. At the same time, TGA indicated enhanced thermal stability at low CMC concentrations, with a maximum decomposition temperature of 326 °C for 1% CMC compared to 315 °C in the control. However, higher loadings (5% CMC) led to slight thermal deterioration, likely due to disruptions in polymer chains. These results confirm that corncob-derived CMC can be successfully integrated into gelatin–chitosan nanofibers to improve structural and thermal properties, positioning them as promising candidates for active food packaging. Future studies will focus on mechanical and antibacterial performance to further validate their practical application.

I. INTRODUCTION

Food packaging plays a crucial role in safeguarding food products against chemical, biological, and physical hazards [1]. Petroleum-based plastics are commonly employed in this field because of their favorable properties, including strong barrier performance, high tensile strength, low weight, and cost-effectiveness [2]. However, their resistance to degradation results in persistent environmental waste and an extended lifespan, both of which contribute to pollution [3]. Consequently, there is growing demand in the food industry for packaging materials that are not only biocompatible and antibacterial but also capable of extending food shelf life [4].

Polymeric nanofibers have been extensively researched in recent years for their potential applications in food packaging [5]. This growing interest is mainly due to their remarkable properties, including a high surface area-to-volume ratio and significant porosity [6]. On top of that, nanofibers offer a key advantage over traditional film-based packaging by effectively encapsulating active agents and micro- and nanocrystals within their porous structure. These nanofibers are mainly produced from synthetic and biopolymeric materials. While synthetic

*Corresponding author. Tel.: +90-533-671-7361; e-mail: yasinakgul@karabuk.edu.tr

petroleum-derived polymers are widely used in food packaging due to their versatility, their application is increasingly restricted due to concerns over non-biodegradability, potential carcinogenic effects, and environmental pollution [7]. Consequently, the demand for cost-effective, biodegradable, and sustainable biopolymeric packaging has become inevitable.

Biodegradable polymers have attracted enormous scientific and industrial interest due to their environmentally friendly aspect [8]. Materials such as chitosan [9], cellulose [10], starch [11], and gelatin [12] have been extensively studied for their potential use in food packaging [13]. Among these, gelatin has drawn particular interest due to its edibility, availability, low cost, biodegradability, and safety [12, 14]. It also exhibits excellent gas barrier properties and controlled water-swelling behavior [15]. However, its poor antibacterial and mechanical properties, along with its high hydrophilicity, limit its use [16]. Therefore, a simple and effective way to address this limitation is by blending gelatin with other polymers and microcrystalline materials. Chitosan, a widely used biopolymer in the food packaging industry, is favored for its non-toxic nature, biodegradability, biocompatibility, and cost-effectiveness. It is an abundant polysaccharide derived from chitin through partial deacetylation, making it a sustainable and functional choice for enhancing packaging materials [17]. Blending chitosan with gelatin nanofibers enhances their antibacterial properties and slightly improves mechanical strength but does not improve surface wettability [18]. For instance, Montaz et al. [19] developed gelatin/chitosan (GEL/CS) bio-nanocomposite films incorporating nickel oxide nanoparticles (NiONPs) synthesized by co-precipitation. The tensile strength increased from 23.83 MPa (neat GEL/CS) to 30.13 MPa with 1% NiONPs. The films exhibited strong antibacterial activity, particularly against *Staphylococcus aureus*, and were non-toxic to fibroblast cells (>88% survival). In another study, Parın, F. N et al. [20] fabricated hydrophilic bioactive nanofibers using a combined electrospinning and electrospraying process with PVA, PVA-Gel, and PVA-Alg as matrices and folic acid (FA) dispersed on fiber surfaces. Characterization confirmed a uniform morphology, stable thermal behavior, and the absence of chemical bonding between FA and polymers. In vitro release studies showed rapid FA release within 8 hours, with release rates influenced by polymer type (49.6% for PVA, 69.55% for PVA-Gel, and 50.88% for PVA-Alg). Cytotoxicity assays (MTT, NRU) using L929 cells demonstrated good biocompatibility, with PVA and PVA-Gel fibers showing higher compatibility than PVA-Alg. These results suggest hybrid nanofibers are promising for fast-release transdermal patch applications, particularly in skin-care products.

Additionally, integrating nano-cellulose and chitosan into gelatin and starch matrices has increased tensile strength, water resistance, and food preservation capabilities [21]. These biodegradable, biocompatible nanocomposite nanofibers offer an eco-friendly alternative to petroleum-based plastics, addressing sustainability concerns while meeting essential packaging requirements. However, natural polymers still face challenges, including lower mechanical strength and greater processing difficulties than synthetic polymers, limiting their broader application [22]. Incorporating nanomaterials, such as cellulose nanocrystals (CNC), offers a promising approach to enhance the performance of natural polymer-based nanofibers. CNC offers high strength and stiffness, low weight, and is both biocompatible and biodegradable. Additionally, CNC appears to positively influence the morphology and diameter of electrospun nanofibers. CNC also positively influences nanofiber morphology and diameter, further improving their properties while maintaining biodegradability [23, 24]. In particular, sourcing cellulose microcrystals (CMC) from agricultural waste, such as corncobs, provides an environmentally conscious, low-cost reinforcement strategy that simultaneously reduces biomass waste while enhancing the functional performance of packaging materials [25].

Significant advancements have been made in nanofiber production, particularly through electrospinning, a technique that uses an electric field to generate fine fibers from polymer solutions or melts. Electrospinning is a versatile method for producing high-quality nanofibers from a wide range of materials. However, it has some limitations, including a low production rate [26]. To address these issues, alternative methods such as melt blowing, which avoids the use of solvents, centrifugal spinning [12], solution blowing [27], and electroblowing [28] are being explored as promising alternatives. Electro-blowing is a novel method for producing nanofibers that uses an electric field in addition to air pressure to enhance fiber production from a solution. The electric field helps uniformly stretch the solution, resulting in higher-quality fibers. Thus, electro-blowing combined the benefits of electrospinning (ES) and solution blowing (SBS) [29]. In the ES technique, a high voltage was applied to form continuous polymer fibers with diameters varying from micrometers to nanometers [30]. While the solution blows, spinning high-compressed air flow drives a polymeric solution [31]. Compared to conventional electrospinning, electro-blowing offers not only improved fiber morphology but also greater scalability, making it a strong candidate for industrial nanofiber fabrication [32].

This study focused on developing a natural nanofiber mat composed of gelatin (G), chitosan (Ch), and corncob-derived cellulose microcrystals (CMC) via electro-blowing to produce materials suitable for food packaging applications. The study primarily emphasizes the fabrication process and structural and thermal characterization of the nanofibers, while evaluations of mechanical strength and hydrophobicity are planned for future work. We hypothesize that blending gelatin and chitosan with corncob-derived CMC processed by electro-blowing will yield nanofibers with superior strength, hydrophobicity, and functional performance compared to conventional blends, thereby offering a sustainable alternative for active food packaging. Initially, the polymer formulations and electro-blowing parameters were systematically optimized. Subsequently, varying concentrations of CMC (1, 3, and 5% w/w) were incorporated into the optimized gelatin–chitosan solution to investigate their influence on the final properties. The fabricated nanofibers were thoroughly characterized using Field Emission Scanning Electron Microscopy (FE-SEM), Attenuated Total Reflectance-Fourier Transform Infrared Spectroscopy (ATR-FTIR), X-ray Diffraction (XRD), Thermogravimetric Analysis (TGA), and air permeability testing to evaluate their potential for food packaging applications.

II. EXPERIMENTAL METHOD / THEORETICAL METHOD

2.1 Materials

Gelatin (Bloom 250–270, Type B), derived from bovine skin, was provided in powder form by Halavet Gida LLC (Istanbul, Türkiye). Chitosan (degree of deacetylation >95%) was obtained from Biyopol (Istanbul, Türkiye). Acetic acid (AA) with 80% purity and a 1.08 g/cm³ density was sourced from Tekkim (Bursa, Türkiye). Formic acid (65%) was purchased from TEKKIM Chemical Industries, Turkey. Corn cobs were collected locally from rural farmers.

2.2 Extraction of Cellulose Microcrystal (CMC) from Corn Cobs

Corn cob residues (3 kg) were collected from rural farmers and air-dried for seven days, followed by oven drying at 45ºC for 24 hours. The cellulose preparation method was based on a previous study with some modifications [33]. After drying, the corn cobs were mechanically ground to produce a fine powder. A portion of this powder

(300 g) was then combined with 1 L of 2% NaOH solution and stirred at 115℃ and 600 rpm for 3 hours using a magnetic stirrer. To safely maintain this temperature, which exceeds the boiling point of the NaOH solution under atmospheric conditions, the alkali pretreatment was carried out in a pressurized reactor (autoclave). Afterward, the mixture was removed from the stirrer and allowed to cool. The powdered material was then oven-dried at 45℃ for 24 hours to reach the desired moisture content and stabilize.

A bleaching solution was prepared consisting of 92% water, 0.7% NaOH, and 6.3% hydrogen peroxide. The pre-treated cellulose was added to this solution, and the mixture was stirred at 700 rpm and 60 °C for 1.5 hours until a homogeneous suspension was obtained. After alkali treatment, the mixture was neutralized using dilute acetic acid and thoroughly washed with distilled water until the filtrate reached neutral pH. The solid residue was then subjected to a bleaching step using a suitable oxidizing agent. During bleaching, the solution pH was adjusted to approximately 4.5 with acetic acid, and the mixture was filtered to remove residual solids. The bleached material was thoroughly washed with distilled water and air-dried for 7 days, yielding corn cob-based cellulose microcrystals. Detailed characterization was conducted on the extracted CMC.

2.3 Solution Preparation

The solution was prepared following the percentage composition detailed in Table 1. To create this solution, 12 wt.% of Gelatin (G) and 3 wt.% of chitosan (Ch)were dissolved in a cosolvent system consisting of 68 wt.% acetic acid and 17 wt.% formic acid. The mixture was stirred continuously with a magnetic stirrer at 60°C for 6 hours to ensure complete dissolution of G and Ch in the solvent mixture. For the preparation of the G-Ch-CMC solution, varying concentrations of cellulose micro-crystals (CMC) at 1, 3, and 5 wt.% were added to the base solution containing 12 wt.% gelatin (G) and 3 wt.% chitosan (Ch) dissolved in the same co-solvent system (68 wt.% acetic acid and 17 wt.% formic acid). This solution was also stirred continuously under similar conditions at 60°C for 4 hours, allowing sufficient time to achieve a uniform, homogeneous blend. Both solutions were prepared to ensure that each component was fully integrated, setting the foundation for further experimental procedures.

Table 1: Design of experiment (DOE)

Sample	Gelatin (%)	Chitosan (%)	Cellulose microcrystal (%)	Acetic Acid (%)	Formic Acid (%)
G-Ch	12	3	0	68	17
G-Ch-1CMC	11.89	2.96	0.15	68	17
G-Ch-3CMC	11.64	2.91	0.45	68	17
G-Ch-5CMC	11.4	2.85	0.75	68	17

2.4 Fabrication of Nanofibers

This study used the electroblowing technique to fabricate nanofiber samples by combining air pressure with an electric field to propel the polymer solution from the nozzle to the collector, as depicted in Figure 1. The nozzle was positioned 47 cm away from the rotating vacuum collector, and an air pressure of 1.5 bar was applied. Simultaneously, an electric voltage of 20 kV was applied at the nozzle tip to enhance solution spinnability and minimize fiber bundling. The polymer solution was fed at a rate of 15 mL/hr, ensuring effective solvent evaporation during its travel from the nozzle to the collector. This process yielded nanofibers with smooth morphologies and varying diameters. The optimized electro-blowing parameters successfully produced uniform nanofibers for the samples designated Gelatin-Chitosan (G-Ch), Gelatin-Chitosan-1% cellulose microcrystal (G-

Ch-1CMC), Gelatin-Chitosan-3% cellulose microcrystal (G-Ch-3CMC), and Gelatin-Chitosan-5% cellulose microcrystal (G-Ch-5CMC). The AREKA aerospinner L1.0 machine was used to produce nanofibers. The optimized set was determined by assessing fiber morphology, uniformity, and the absence of beads using SEM. For example, the gelatin–chitosan blend solution was first tested over a polymer concentration range of 10–16 wt%, with applied voltages of 15-35 kV and airflow pressures of 0.5-1.5 Bar. The optimized parameters were selected based on their ability to yield continuous, bead-free fibers with uniform diameters.

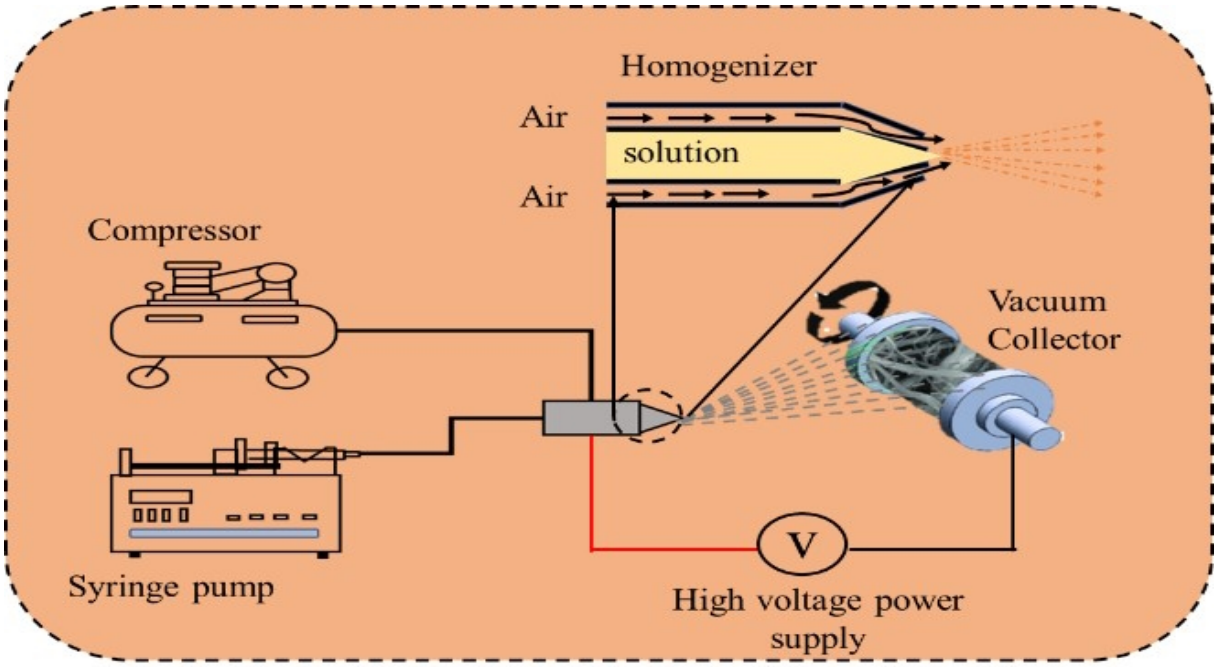

Figure 1. Schematic drawing of the electro-blowing fiber production method

2.5. Characterization Methods

2.5.1 Scanning electron microscope (SEM)

A Carl Zeiss Ultra Plus Field Emission Scanning Electron Microscope (FE-SEM) was used to examine the structures of the fibrous mats. ImageJ software was used to process the SEM images, enabling calculation of the average nanofiber diameter and its distribution. One hundred diameter measurements were taken from randomly selected images for each sample. The average fiber diameter was calculated from multiple SEM images using ImageJ software, while the fiber diameter distribution was analyzed with OriginLab software, as shown in Figure 2.

2.5.2 FTIR

To assess interactions among components within the fibrous mats, Fourier-transform infrared (FTIR) spectra were obtained using a Bruker ALPHA FTIR Spectrometer. This process involved capturing detailed spectral data to identify characteristic functional groups and molecular bonds present in the samples. A total of 24 scans were recorded for each sample, covering a broad wavelength range from 400 to 4000 cm^{-1}. This range provided

comprehensive insight into the chemical structure and potential interactions among the components within the mats.

2.5.3. Thermogravimetric analysis (TGA)

To examine the thermal stability and degradation patterns of the nanofiber mat, thermogravimetric analysis (TGA) was conducted using a Hitachi STA 7300 thermogravimetric analyzer (Hitachi, Japan). This analysis provided insights into the material's behavior under heat, indicating its potential performance and resilience in applications exposed to varying temperatures. During the TGA, the samples were heated from room temperature to 550 °C at a controlled rate of 10 °C/min. A steady nitrogen gas flow of 2 mL/min was maintained throughout heating to prevent oxidation and ensure a stable, inert environment. This setup enabled precise observation of weight-loss stages and thermal decomposition characteristics, shedding light on the material's composition and degradation profile at elevated temperatures.

2.5.4. Air permeability

The air permeability of the gelatin nanofiber mats was evaluated using a Prowhite Air Test II apparatus to determine their breathability and suitability for applications requiring controlled airflow. This assessment was conducted at a controlled temperature of 25 ℃ within a designated circular area of 50 mm in diameter on each sample, ensuring consistency across all measurements. During each test, a steady air pressure of 100 Pa was applied to the mat, and the apparatus recorded the rate of air passage through the nanofiber structure. This setup enabled precise measurement of air permeability, providing insight into the material’s porosity and potential applications in filtration, protective barriers, and breathable packaging.

III. RESULTS AND DISCUSSIONS

3.1 Characterization results of CMCs

3.1.1. SEM

The image in Figures 2(a) and (b) reveals a distinct contrast between untreated and treated corn cob samples. In image (a), the raw corn cob surface appears rough, with irregular particle sizes and orientations. This texture reflects the presence of structural components like lignin, hemicellulose, and pectin, which contribute to the rigidity of the plant cell wall. Following chemical pre-treatment and hydrolysis, image (b) displays a smoother, more uniform surface with a noticeable sheen. This transformation results from the effective removal of non-cellulosic materials during treatment. The resulting structure is indicative of microcrystalline cellulose, characterized by increased homogeneity and clarity. The comparison between the two images confirms that the pre-treatment process successfully modified the native corn cob structure, producing a refined cellulose material. The successful removal of hemicelluloses, lignin, and pectins resulted in a purified structure, as evidenced by the SEM (Figure 2(c)) image showing the characteristic morphology of microcrystalline cellulose.

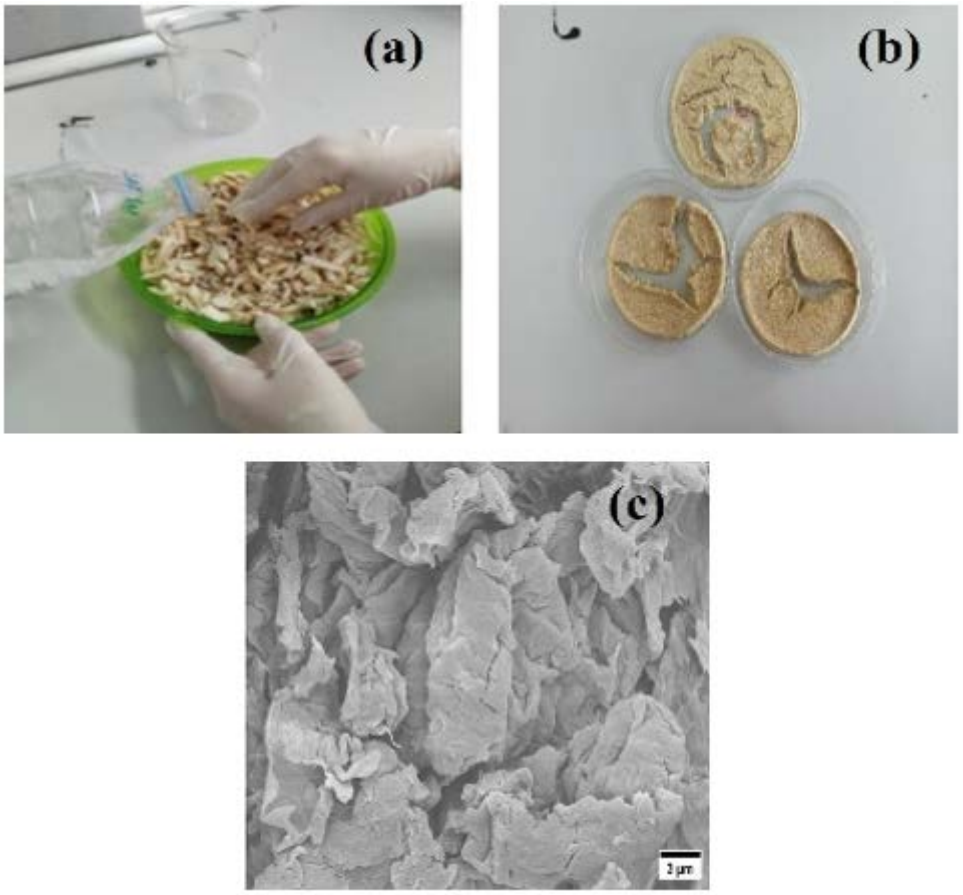

Figure 2. Images of the raw corn cob (a), isolated (b), and the SEM (c)image of CMC

3.1.2. FTIR

Figure 3(a) shows the FTIR spectra of corn cob, alkaline-treated material, bleached cellulose, and acid-hydrolyzed cellulose. A broad band between 3340–3420 cm^{-1} corresponds to the stretching vibrations of hydrogen-bonded hydroxyl (OH) groups, while peaks around 2920 cm^{-1} are attributed to C–H stretching. In the raw biomass, the OH-related peak appears weaker due to the presence of non-cellulosic components such as waxes, hemicellulose, and lignin, which limit the exposure of hydroxyl groups. A faint shoulder around 1730 cm^{-1} indicates the presence of acetyl and uronic ester groups from trace amounts of hemicellulose. This feature disappears after alkali treatment, confirming the effective removal of hemicellulose using a 2% w/v NaOH solution [34].

The absorption band near 1640 cm^{-1} is associated with the OH bending of adsorbed water, reflecting the exposure of hydroxyl groups. The peak at 1430 cm^{-1}, linked to CH_2 bending, is characteristic of the crystalline structure in cellulose. Meanwhile, the signal at 1372 cm^{-1} corresponds to CH and CO bond bending in the aromatic rings of polysaccharides [35]. A distinct peak at 1254 cm^{-1} is due to CO out-of-plane stretching in lignin's aryl groups [36]. Additionally, all samples exhibit a band around 899 cm^{-1}, which corresponds to glycosidic CH deformation and OH bending, markers of β-glycosidic linkages in cellulose chains [33].

3.1.3. TGA

Thermogravimetric analysis (TGA) and derivative thermogravimetry (DTG) were used to analyze the thermal decomposition behavior of the isolated cellulose microcrystal (CMC). The corresponding TGA curve is presented

in Figure 3(b). An initial weight loss of approximately 9 wt% occurred between 30°C and 105°C across all samples, primarily due to moisture evaporation. A maximum decomposition was observed near 326°C, likely associated with the release of low-molecular-weight residues left over from the isolation process. The most significant mass loss was recorded between 250°C and 400°C, marking the main phase of thermal degradation. This range corresponds to the decomposition of organic constituents such as cellulose and remaining hemicellulose or lignin [36].

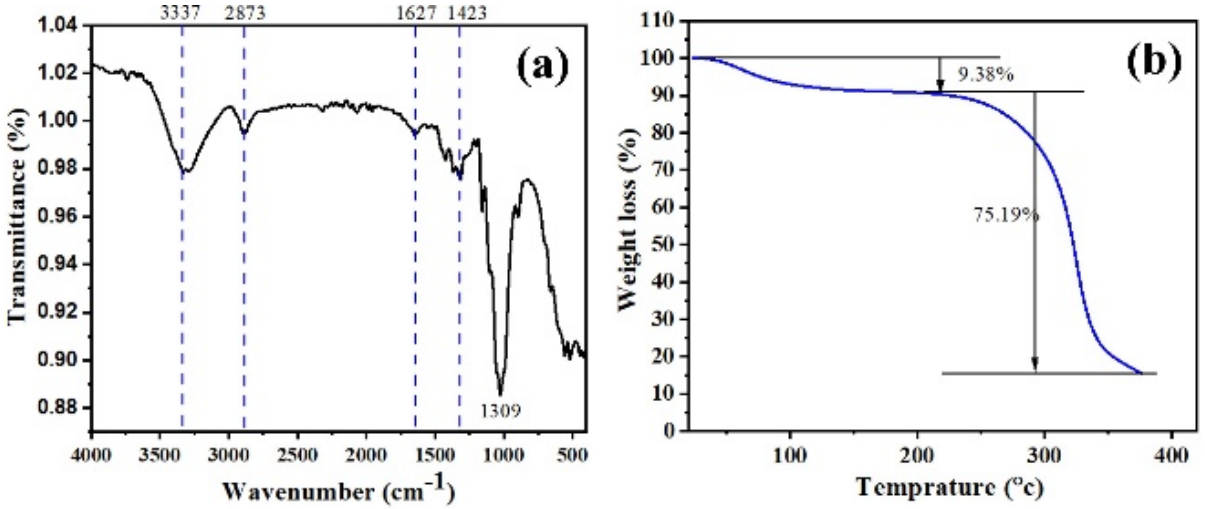

Figure 3. FTIR (a) and TGA(b) results of CMC

3.2 Characterization Results of Nanofibrous Mats

3.2.1. SEM analysis

The surface morphologies of G-Ch and G-Ch-1CMC, G-Ch-3CMC, and G-Ch-5CMC micro-nanofibrous mats were analyzed using scanning electron microscopy (SEM). The resulting SEM images and the fiber diameter distributions for each sample are presented in Figure 4. All SEM images were captured at two magnification levels: 1000× (low) and 5000× (high). The incorporation of cellulose microcrystals (CMC) into gelatin/chitosan nanofibers profoundly influences their morphology and fiber diameter, which are critical for optimizing performance in food packaging applications. As shown in Figure 4(a)&(b), with the addition of one percent CMC, there was a slight increment in fiber diameter from 642.19 ± 40.36 nm to 699 ± 20.32 nm. This might be due to the high crystallinity of cellulose microcrystals, which enables them to function as reinforcing agents within the nanofiber matrix and affects structural integrity [37]. Furthermore, the interaction between chitosan and CMCs, driven by electrostatic and hydrogen bonding, modifies the solution's rheological properties, enhancing dispersion and stability during fiber production [38].

Increasing the CMC concentration to 3% further reduced the fiber diameter to 524.39 ± 38.18 nm. This reduction may be attributed to improved solution conductivity during electro-blowing, which enhances polymer chain alignment and jet stretching, leading to finer fibers. Similar findings were reported by Amini et al. [39], who observed that low CMC concentrations reduce fiber diameter by increasing solution conductivity during electrospinning. The SEM analysis revealed that increasing CMC content slightly reduced the average fiber diameter. While this effect is often attributed to enhanced solution conductivity and reduced viscosity, no direct

conductivity or viscosity measurements were performed in the present study. Therefore, the proposed mechanism remains a qualitative explanation. Similar trends have been reported in previous studies, where the addition of cellulose microcrystals or other ionic fillers increased solution conductivity, resulting in thinner fibers during electrospinning or electro-blowing [40]. Future investigations will include systematic measurements of solution conductivity and viscosity to quantitatively confirm this mechanism and provide a more complete understanding of CMC's influence on fiber formation. This enhancement facilitates polymer chain alignment and jet stretching, as demonstrated in studies on biopolymer blends. However, exceeding 5% CMC increases solution viscosity, leading to thicker fibers or irregular morphologies due to restricted polymer flow, a phenomenon corroborated by DE Sameen et al. [41]. This study focuses on optimizing the electrospinning parameters.

Morphologically, well-dispersed CMC stabilizes the electrospinning jet, improving fiber uniformity and minimizing bead formation. In contrast, excessive CMC loading can lead to defects such as fiber branching or aggregation, as reported by Kumar et al. [42] for nanocellulose-reinforced composites. These effects result from a balance between conductivity-driven fiber thinning and viscosity-induced resistance, along with interfacial hydrogen bonding between CMC's hydroxyl groups and gelatin/chitosan, which enhances matrix compatibility. For food packaging applications, optimally tuned CMC concentrations yield thinner, more uniform fibers that enhance oxygen and moisture barrier properties through denser packing. Recent advancements emphasize the role of dispersion techniques, such as sonication in acetic acid, and precise parameter adjustments, such as lower flow rates for high-viscosity blends, to minimize defects and enable the scalable production of biodegradable, high-performance nanofiber mats. Overall, these findings highlight CMC's potential in eco-friendly packaging, provided its concentration and processing conditions are carefully optimized to balance structural integrity and functional performance.

3.2.2. FTIR analysis

FTIR spectroscopy was employed to analyze the nanofibers and investigate potential interactions between the polymers. Figure 5(a) presents the FTIR spectra of G-Ch, G-Ch-1CMC, G-Ch-3CMC, and G-Ch-5CMC nanofibrous mats. Key absorption bands were identified to facilitate comparison between the different samples. In the FTIR spectrum of CMC powder, the bands observed between 3300–3400 cm^{-1} and 2800–2900 cm^{-1} correspond to the stretching vibrations of O-H and C-H groups, respectively. Additionally, peaks at 1645 cm^{-1}, 1418 cm^{-1}, and 1321 cm^{-1} are associated with OH bending of adsorbed water, symmetric CH_2 bending, and the bending vibrations of C-H and C-O groups in polysaccharide rings, respectively [43–45].

The FTIR spectrum of G-Ch, G-Ch-1CMC, G-Ch-3CMC, and G-Ch-5CMC nanofibers revealed characteristic peaks from both polymers. The bands at 1633 cm^{-1} and 1537 cm^{-1} correspond to the N-H stretching vibrations of amide I and II, respectively, while the peak at 1242 cm^{-1} is attributed to amide III [46]. FTIR spectra of chitosan-gelatin nanofibers at varying concentrations revealed that increasing chitosan content enhanced the intensity of the absorption band in the 1155–1025 cm^{-1} region, corresponding to C–O stretching vibrations in the glycosidic bonds of chitosan's polysaccharide structure [47]. Additionally, this peak shifted to a lower wavenumber, suggesting hydrogen bond formation between gelatin and chitosan within the nanofibers. Additionally, the increased intensity of the band around 3200–3500 cm^{-1} indicates strong molecular compatibility, likely due to hydrogen bonding between the polymers. This analysis confirms that the characteristic bands of G and Ch remain present in the G-Ch nanofibers, supporting the miscibility of these components after the spinning process [44].

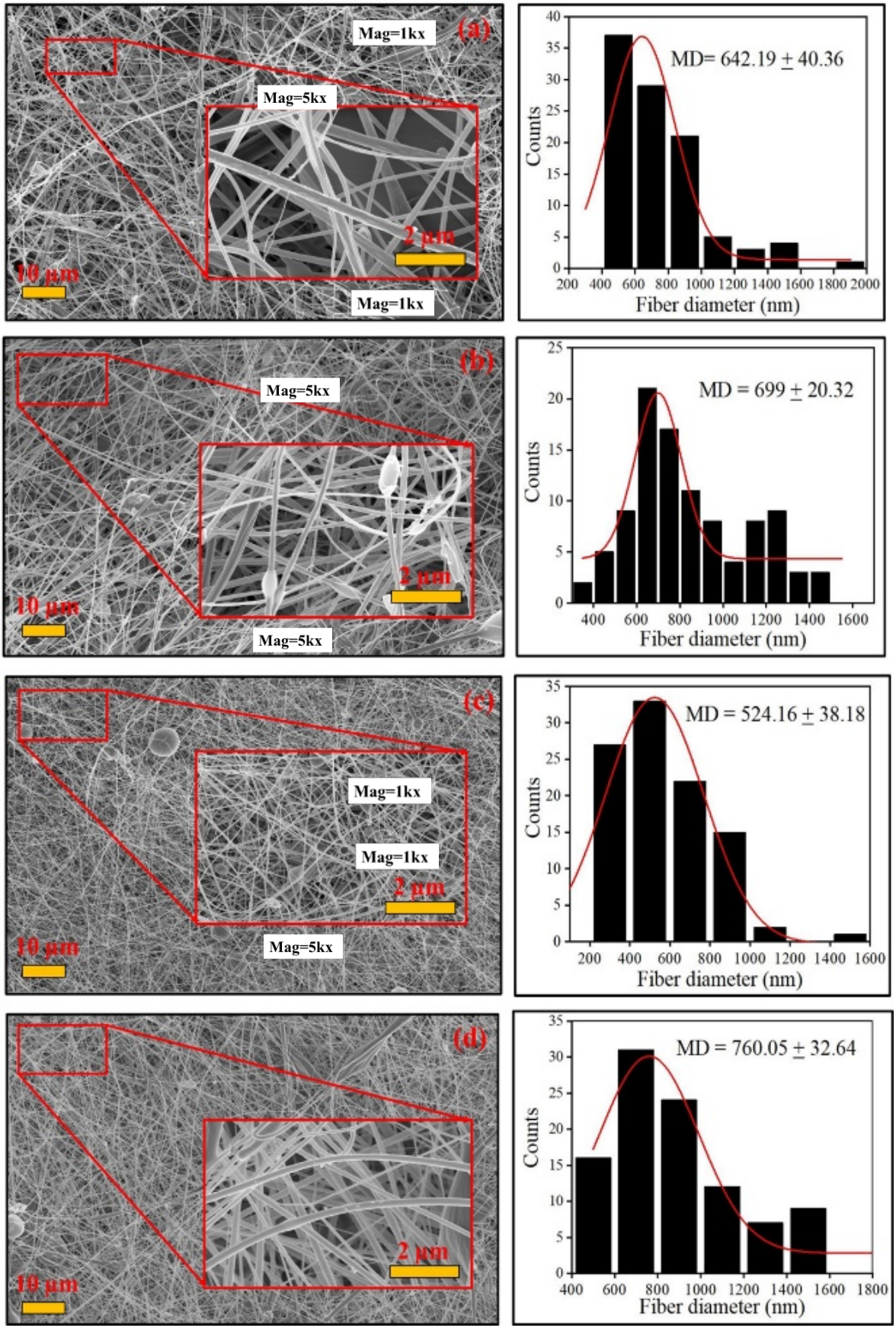

Figure 4. SEM images at lower (1,000×) and higher (5,000×) magnifications, along with fiber diameter distributions, for G–Ch (a), G–Ch–1CMC (b), G–Ch–3CMC (c), and G–Ch–5CMC (d) nanofibrous mats

3.2.3. Thermal analysis

The thermal stability of nanofiber mats is crucial for food packaging, as it ensures structural integrity and functionality across varying temperatures. Figure 5(b) presents the TGA result of nanofiber mats. Their resistance to decomposition at high temperatures enhances durability, making them practical for long-term use[48]. TGA analysis was conducted to assess the thermal stability of the developed nanofibers. Thermogravimetric analysis (TGA) curves of G-Ch nanofibers with varying CMC concentrations are shown in Figure 3(b), which reveal two primary weight-loss stages between 30 °C and 450 °C. The first stage, occurring between 30–152 ºC, is associated with the evaporation of absorbed water and residual acetic acid retained within the nanofiber structure [49]. The second stage, observed between 210–400 ºC, corresponds to the thermal decomposition of G and Ch polymeric chains, resulting in approximately 53.78% weight loss [50]. As observed in Figure 3(b), thermal stability improves with the addition of 1% CMC but declines at 3% and 5% CMC concentrations. This could be due to moderate CUR levels (≤ 1%) enhancing fiber stability through intermolecular hydrogen bonding. In comparison, excessive CMC (>3%) disrupts polymeric chain rearrangement and crystallization, weakening the compact G-Ch matrix structure[44]. This suggests that CMC incorporation has little effect on the thermal degradation pattern, confirming its stable integration within the nanofiber matrix [51].

3.2.4. XRD analysis

The relative amounts of crystalline and amorphous regions in the cellulose samples (native corn cob cellulose (NC), corn cob cellulose acetates (CA, CDA), and a commercial brand of cellulose acetate (CCA)) were determined by Azubuike from the PXRD diffractograms using Diffrac Suite Eva software, and the result is summarized in Table 2 [52].

Table 2. Degree of Crystallinity generated from the XRD diffractograms [52]

Sample	Crystallinity (%)	Amorphous (%)
NC	42.8	57.2
CA	29.3	70.7
CDA	22.4	77.6
CCA	10.0	90.0

X-ray diffraction (XRD) analysis was performed to examine the crystalline structure of the nanofiber membranes, as shown in Figure 3(c). The XRD patterns reveal no distinct crystal peaks, confirming the amorphous nature of the membranes. A broad diffraction peak at approximately 21° is characteristic of gelatin-chitosan composite membranes. This peak likely corresponds to the triple-helical crystalline structure of collagen with a 1.1 nm periodicity, the random-coil conformation of macromolecules, or the semicrystalline nature of biopolymers [53, 54]. The XRD patterns of membranes with varying CMC content are similar to those without CMC, suggesting that CMC does not significantly affect crystallinity. Similar findings were reported by Jun Chean et al.[55], who developed an acellular gelatin-chitosan-cellulose nanocrystal (GCCNC) scaffold as a potential wound dressing and analyzed its crystallographic structure using X-ray diffraction (XRD). Their study found that the G10CNC scaffold exhibited higher intensity, indicating the successful incorporation of CNCs. However, the C10CNC scaffold showed reduced intensity despite containing the same amount of CNCs, which was attributed to genipin crosslinking, altering the semi-crystalline structure of chitosan. Additionally, all GCCNC scaffolds were amorphous, with G3C7CNC being the most amorphous. These findings support our results, highlighting the

influence of CNCs and crosslinking on scaffold crystallinity, which plays a critical role in material properties for food packaging applications.

3.2.5. Air permeability

The air permeability results presented in Figure 5(d) demonstrate a progressive increase in permeability with the addition of cellulose microcrystal (CMC) to the G-Ch matrix. The pure G-Ch sample exhibited the lowest air permeability, approximately 2.0 mm/s, indicating a relatively dense and compact structure. Introducing 1% CMC (G-Ch-1CMC) led to a slight increase in air permeability, while further increases to 3% and 5% CMC (G-Ch-3CMC and G-Ch-5CMC) resulted in more substantial improvements, with values reaching approximately 2.6 ± 0.9 mm/s. This trend suggests that higher CMC loading promotes a more open network within the material, facilitating easier air flow. The flexible chains of CMC likely interfere with the dense packing of the chitosan matrix, creating microvoids and channels that enhance permeability. This behavior aligns with findings reported by Ahuja et al. [56], who showed that gelatin–chitosan films with 1–5 wt% microcrystalline cellulose exhibited 10–30% higher air permeability than neat films, an effect attributed to MCC aggregation and the formation of micro-voids under standard casting conditions. These findings support the notion that CMC acts as a porosity enhancer when combined with biopolymers like chitosan. Overall, the observed increase in air permeability with higher CMC content confirms that CMC incorporation effectively modulates the air transport properties of G-Ch composites. This enhancement could be particularly valuable for applications that require breathability, such as filtration membranes, wound dressings, and biodegradable packaging materials.

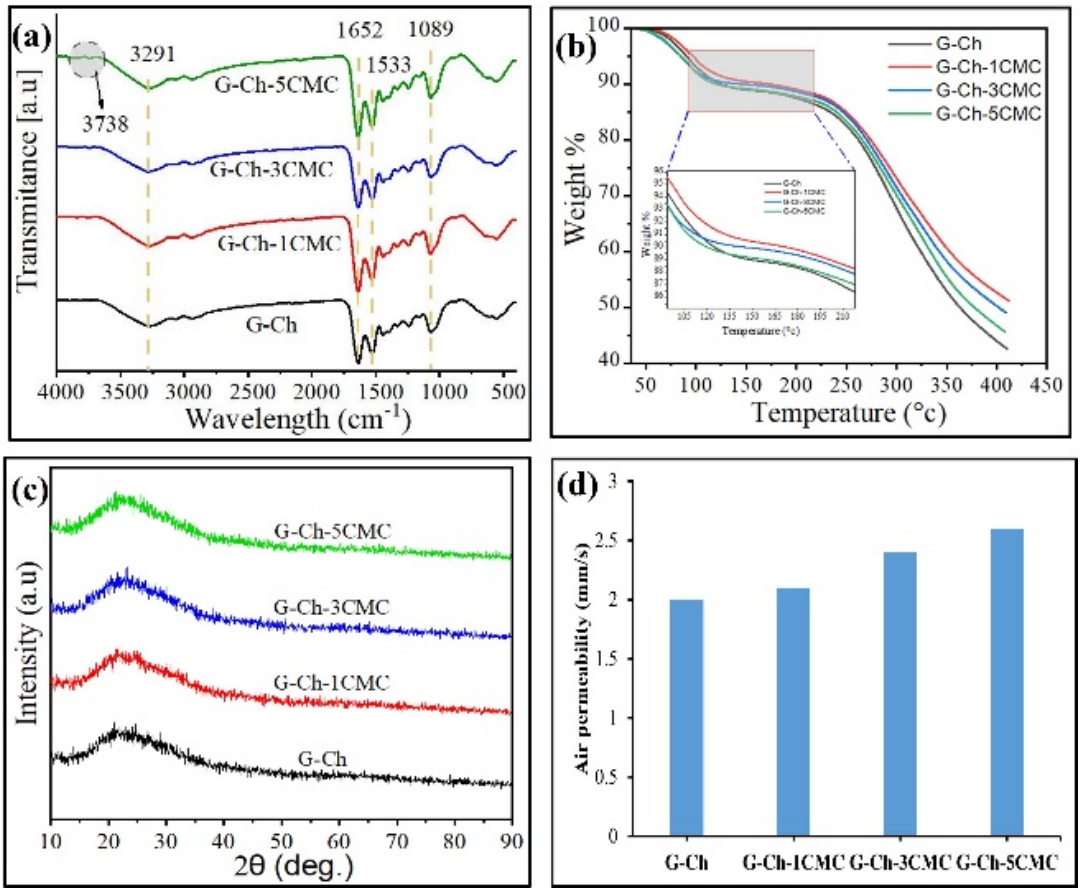

Figure 5. FTIR spectroscopy (a), TGA (b), XRD (c), and air permeability (d) analysis of G-Ch, G-Ch-1CMC, G-Ch-3CMC, and G-Ch-5CMC nanofiber mats

IV. CONCLUSIONS

This study demonstrated the successful fabrication of biodegradable nanofiber mats comprising gelatin, chitosan, and corncob-derived cellulose microcrystals (CMC) via electro-blowing. The incorporation of chitosan improved the antibacterial potential of gelatin, while the addition of CMC significantly enhanced fiber morphology and thermal stability. SEM analysis confirmed uniform, bead-free fibers with average diameters ranging from 642.19 ± 40.36 nm to 760.05 ± 32.64 nm, and the water contact angle increased with higher CMC loading, indicating improved surface hydrophobicity. Notably, incorporation of 1 wt% CMC resulted in enhanced thermal stability, whereas higher concentrations led to slight deterioration, likely due to agglomeration. Compared to conventional electrospinning, the electro-blowing technique provided uniform fibers with higher production efficiency and greater scalability, marking a key advantage of this work over previous studies.

These findings highlight the novelty of combining natural polymers with corncob-derived CMC via electro-blowing to create an environmentally friendly packaging material. However, the observed increase in air permeability at higher CMC contents indicates the need for further optimization. Although mechanical and antibacterial tests were outside the scope of the present study, they represent critical parameters for food packaging applications and will be the focus of future investigations. Overall, the developed gelatin–chitosan–CMC nanofibers offer a promising pathway toward scalable, sustainable, and functional active food packaging solutions.

ACKNOWLEDGMENT

This study was supported by the TUBITAK 2209-A program.

REFERENCES

1. Kalpana S, Priyadarshini S, Leena MM, Moses J, Anandharamakrishnan C (2019) Intelligent packaging: Trends and applications in food systems. Trends Food Sci Technol 93:145–157. https://doi.org/10.1016/j.tifs.2019.09.008
2. Reichert CL, Bugnicourt E, Coltelli MB, Cinelli P, Lazzeri A, Canesi I, et al (2020) Bio-based packaging: Materials, modifications, industrial applications and sustainability. Polymers 12(7):1558. https://doi.org/10.3390/polym12071558
3. Haghighi H, Leugoue SK, Pfeifer F, Siesler HW, Licciardello F, Fava P, Pulvirenti A (2020) Development of antimicrobial films based on chitosan-polyvinyl alcohol blend enriched with ethyl lauroyl arginate (LAE) for food packaging applications. Food Hydrocolloids, 100:105419. https://doi.org/10.1016/j.foodhyd.2019.105419
4. Han J, Ruiz-Garcia L, Qian J, Yang X (2018) Food packaging: A comprehensive review and future trends. Compr Rev Food Sci Food Saf 17(4):860–877. https://doi.org/10.1111/1541-4337.12343
5. Min T, Zhou L, Sun X, Du H, Zhu Z, Wen Y (2022) Electrospun functional polymeric nanofibers for active food packaging: A review. Food Chem 391:133239. https://doi.org/10.1016/j.foodchem.2022.133239
6. Gulzar S, Tagrida M, Prodpran T, Benjakul S (2022) Antimicrobial film based on polylactic acid coated with gelatin/chitosan nanofibers containing nisin extends the shelf life of Asian seabass slices. Food Packag Shelf Life 34:100941. https://doi.org/10.1016/j.fpsl.2022.100941
7. Amjadi S, Emaminia S, Davudian SH, Pourmohammad S, Hamishehkar H, Roufegarinejad L (2019) Preparation and characterization of gelatin-based nanocomposite containing chitosan nanofiber and ZnO nanoparticles. Carbohydr Polym, 216:376–384. https://doi.org/10.1016/j.carbpol.2019.03.062
8. Wu F, Misra M, Mohanty AK (2021) Challenges and new opportunities on barrier performance of biodegradable polymers for sustainable packaging. Prog Polym Sci 117:101395. https://doi.org/10.1016/j.progpolymsci.2021.101395

9. Arkoun M, Daigle F, Heuzey MC Ajji A (2017) Mechanism of action of electrospun chitosan-based nanofibers against meat spoilage and pathogenic bacteria. Molecules 22(4):585. https://doi.org/10.3390/molecules22040585
10. Balasubramaniam SL, Patel AS, Nayak B (2020) Surface modification of cellulose nanofiber film with fatty acids for developing renewable hydrophobic food packaging. Food Packag Shelf Life 26:100587. https://doi.org/10.1016/j.fpsl.2020.100587
11. Fonseca LM, dos Santos Cruxen CE, Bruni GP, Fiorentini ÂM, da Rosa Zavareze E, Lim LT, Dias ARG (2019) Development of antimicrobial and antioxidant electrospun soluble potato starch nanofibers loaded with carvacrol. Int J Biol Macromol 139:1182–1190. https://doi.org/10.1016/j.ijbiomac.2019.08.096
12. Doğan N, Doğan C, Eticha AK, Gungor M, Akgul Y (2022) Centrifugally spun micro-nanofibers based on lemon peel oil/gelatin as novel edible active food packaging: Fabrication, characterization, and application to prevent foodborne pathogens E. coli and S. aureus in cheese. Food Control 139:109081. https://doi.org/10.1016/j.foodcont.2022.109081
13. Flórez M, Guerra-Rodríguez E, Cazón P, Vázquez M (2022) Chitosan for food packaging: Recent advances in active and intelligent films. Food Hydrocolloids 124:107328. https://doi.org/10.1016/j.foodhyd.2021.107328
14. Etichab AK, Akgul Y (2024) Optimization of gelatin nanofibrous webs fabricated via electrically assisted solution blow spinning for air filtration applications. Int J Environ Sci Technol 1–18. https://doi.org/10.1007/s13762-024-05482-2
15. Lu Y, Luo Q, Chu Y, Tao N, Deng S, Wang L, Li L (2022) Application of gelatin in food packaging: A review. Polymers 14(3):436. https://doi.org/10.3390/polym14030436
16. Zhang X, Do MD, Casey P, Sulistio A, Qiao GG, Lundin L, … Kosaraju, S. (2010) Chemical Modification of Gelatin by a Natural Phenolic Cross-linker, Tannic Acid. J Agric Food Chem 58(11):6809–6815. https://doi.org/10.1021/jf1004226
17. Gulzar S, Tagrida M, Nilsuwan K, Prodpran T, Benjakul S (2022) Electrospinning of gelatin/chitosan nanofibers incorporated with tannic acid and chitooligosaccharides on polylactic acid film: Characteristics and bioactivities. Food Hydrocolloids 133:107916. https://doi.org/10.1016/j.foodhyd.2022.107916
18. Akhouy G, Eticha A K, Dogan C, Dogan N, Calisir M D, Toptas A, … Akgul Y (2024) Electro-blown micro-nanofibrous mats with Origanum elongatum essential oil for enhancing the shelf life of tomato (Solanum lycopersicum). Int J Food Sci Technol 17600. https://doi.org/10.1111/ijfs.17600
19. Momtaz M, Momtaz E, Mehrgardi MA, Momtaz F, Narimani T, Poursina F (2024) Preparation and characterization of gelatin/chitosan nanocomposite reinforced by NiO nanoparticles as an active food packaging. Sci Rep 14(1):519. https://doi.org/10.1038/s41598-023-50260-8
20. Parın FN, Ullah A, Yeşilyurt A, Parın U, Haider MK, Kharaghani D (2022) Development of PVA–psyllium husk meshes via emulsion electrospinning: Preparation, characterization, and antibacterial activity. Polymers 14(7):1490. https://doi.org/10.3390/polym14071490
21. Noorbakhsh-Soltani SM, Zerafat MM, & Sabbaghi S (2018) A comparative study of gelatin and starch-based nano-composite films modified by nano-cellulose and chitosan for food packaging applications. Carbohydr Polym 189:48–55. https://doi.org/10.1016/j.carbpol.2018.02.012
22. Bombin ADJ, Dunne NJ, McCarthy HO (2020) Electrospinning of natural polymers for the production of nanofibres for wound healing applications. Mater Sci Eng C 114:110994. https://doi.org/10.1016/j.msec.2020.110994
23. Kargarzadeh H, Mariano M, Huang J, Lin N, Ahmad I, Dufresne A, Thomas S (2017) Recent developments on nanocellulose reinforced polymer nanocomposites: A review. Polymer 132:368–393. https://doi.org/10.1016/j.polymer.2017.09.043
24. Zhou C, Chu R, Wu R, Wu Q (2011) Electrospun Polyethylene Oxide/Cellulose Nanocrystal Composite Nanofibrous Mats with Homogeneous and Heterogeneous Microstructures. Biomacromolecules 12(7):2617–2625. https://doi.org/10.1021/bm200401p
25. Gómez-García R, Sousa SC, Ramos ÓL, Campos, DA, Aguilar, CN, Madureira, AR, Pintado, M (2024) Obtention and characterization of microcrystalline cellulose from industrial melon residues following a biorefinery approach. Molecules 29(14):3285. https://doi.org/10.3390/molecules29143285
26. Wei Z (2018). Research process of polymer nanofibers prepared by melt spinning. IOP Conf Ser: Mater Sci Eng 452:022002, IOP Publishing. https://doi.org/10.1088/1757-899X/452/2/022002
27. Abi J, Ahmed SB, Dogan C, Dogan N, Akgul (2024) Production and Characterization of Electro-Blown Nanofibers Incorporated with Pine Pollen for Fast-Dissolving Tablet Applications. Available at SSRN 4768545. Retrieved from https://doi.org/10.1016/j.jddst.2024.106222
28. Parin F, Ullah S, Yildirim K, Hashmi M, & Kim I (2021) Fabrication and Characterization of Electrospun Folic Acid/Hybrid Fibers: In Vitro Controlled Release Study and Cytocompatibility Assays, Polymers (Basel) 13 (2021). https://doi.org/10.3390/polym13203594

29. Eticha AK, Toptaş A, Akgül Y, Kiliç A (2023) Electrically assisted solution blow spinning of PVDF/TPU nanofibrous mats for air filtration applications. Turk J Chem 47(1):47–53. https://doi.org/10.55730/1300-0527.3515
30. Akhouy G, Aziz K, Gebrati L, El Achaby M, Akgul Y, Yap PS., … Aziz F (2023) Recent applications on biopolymers electrospinning: strategies, challenges and way forwards. Polym-Plast Technol Mater 1–22. https://doi.org/10.1080/25740881.2023.2234459
31. Dadol GC, Kilic A, Tijing LD, Lim KJA, Cabatingan LK, Tan NPB, … Polat Y (2020) Solution blow spinning (SBS) and SBS-spun nanofibers: Materials, methods, and applications. Mater Today Commun, 25:101656. https://doi.org/10.1016/j.mtcomm.2020.101656
32. Ahmed SB, Doğan N, Akgul Y, Doğan C (2025) Functional Bio-Nanofibers for Active Packaging: Electro-Blown Gelatin/Xanthan Gum with Carbon Dots. Bionanoscience 15(3):338. https://doi.org/10.1007/s12668-025-01929-z
33. Singh HK, Patil T, Vineeth SK, Das S, Pramanik A, Mhaske ST (2020) Isolation of microcrystalline cellulose from corn stover with emphasis on its constituents: corn cover and corn cob. Mater Today Proc, 27:589–594. https://doi.org/10.1016/j.matpr.2019.12.065
34. Thomas MG, Abraham E, Jyotishkumar P, Maria HJ, Pothen LA, Thomas S (2015) Nanocelluloses from jute fibers and their nanocomposites with natural rubber: Preparation and characterization. Int J Biol Macromol 81:768–777. https://doi.org/10.1016/j.ijbiomac.2015.08.053
35. Naduparambath S, Jinitha TV, Shaniba V, Sreejith MP, Balan AK, Purushothaman E (2018) Isolation and characterisation of cellulose nanocrystals from sago seed shells. Carbohydr Polym 180:13–20. https://doi.org/10.1016/j.carbpol.2017.09.088
36. Moriana R, Vilaplana F, Ek M (2016) Cellulose nanocrystals from forest residues as reinforcing agents for composites: a study from macro-to nano-dimensions. Carbohydr Polym 139:139–149. https://doi.org/10.1016/j.carbpol.2015.12.020
37. Morsi M, Oraby A, Elshahawy A, Abd El-Hady R (2019) Preparation, structural analysis, morphological investigation and electrical properties of gold nanoparticles filled polyvinyl alcohol/carboxymethyl cellulose blend. J Mater Res Technol 8(6):5996–6010. https://doi.org/10.1016/j.jmrt.2019.09.074
38. Li Z, Mei S, Dong Y, She F, Kong L (2019) High efficiency fabrication of chitosan composite nanofibers with uniform morphology via centrifugal spinning. Polymers 11(10):1550. https://doi.org/10.3390/polym11101550
39. Abdollahi A, Roghani-Mamaqani H, Salami-Kalajahi M, Razavi B, Sahandi-Zangabad K (2020). Encryption and optical authentication of confidential cellulosic papers by ecofriendly multi-color photoluminescent inks. Carbohydr Polym 245:116507. https://doi.org/10.1016/j.carbpol.2020.116507
40. Ismaili D, Parın FN, Sıcak Y, Öztürk M, Terzioğlu P (2024) Electrospun lavender essential oil-loaded polylactic acid nanofibrous mats for antioxidant applications. Polym Bull 81(15):13975–13992. https://doi.org/10.1007/s00289-024-05370-2
41. Sameen DE, Ahmed S, Lu R, Li R, Dai J, Qin W, … Liu Y (2022) Electrospun nanofibers food packaging: trends and applications in food systems. Crit. Rev. Food Sci Nutr 62(22):6238–6251. https://doi.org/10.1080/10408398.2021.1899128
42. Gong X, Kalantari M, Aslanzadeh S, Boluk Y (2022) Interfacial interactions and electrospinning of cellulose nanocrystals dispersions in polymer solutions: a review. J. Dispersion Sci Technol 43(7):945–977. https://doi.org/10.1080/01932691.2020.1847137
43. Kargarzadeh H, Sheltami RM, Ahmad I, Abdullah I, Dufresne A (2015) Cellulose nanocrystal: A promising toughening agent for unsaturated polyester nanocomposite. Polymer 56:346–357. https://doi.org/10.1016/j.polymer.2014.11.054
44. Habibi S, Hajinasrollah K (2018) Electrospinning of nanofibers based on chitosan/gelatin blend for antibacterial uses. Russ J Appl Chem 91(5):877–881. https://doi.org/10.1134/S1070427218050191
45. Hivechi A, Bahrami SH, Siegel RA (2019) Drug release and biodegradability of electrospun cellulose nanocrystal reinforced polycaprolactone. Mater Sci Eng C 94:929–937. https://doi.org/10.1016/j.msec.2018.10.037
46. Jalaja K, Naskar D, Kundu SC, James NR (2016) Potential of electrospun core–shell structured gelatin–chitosan nanofibers for biomedical applications. Carbohydr Polym 136:1098–1107. https://doi.org/10.1016/j.carbpol.2015.10.014
47. Kumar S, Mudai A, Roy B, Basumatary IB, Mukherjee A, Dutta J (2020) Biodegradable hybrid nanocomposite of chitosan/gelatin and green synthesized zinc oxide nanoparticles for food packaging. Foods 9(9):1143. https://doi.org/10.3390/foods9091143
48. Duan M, Sun J, Huang Y, Jiang H, Hu Y, Pang J, Wu C (2023) Electrospun gelatin/chitosan nanofibers containing curcumin for multifunctional food packaging. Food Sci Hum Wellness 12(2):614–621. https://doi.org/10.1016/j.fshw.2022.07.064

49. Rojas A, Velasquez E, Pina C, Galotto MJ, de Dicastillo CL (2021) Designing active mats based on cellulose acetate/polycaprolactone core/shell structures with different release kinetics. Carbohydr Polym 261:117849. https://doi.org/10.1016/j.carbpol.2021.117849
50. Liu Y, Qin Y, Bai R, Zhang X, Yuan L, Liu J (2019) Preparation of pH-sensitive and antioxidant packaging films based on κ-carrageenan and mulberry polyphenolic extract. Int J Biol Macromol 134:993–1001. https://doi.org/10.1016/j.ijbiomac.2019.05.175
51. Ribeiro AS, Costa SM, Ferreira DP, Abidi H, Fangueiro R (2021) Development of chitosan-gelatin nanofibers with cellulose nanocrystals for skin protection applications. Key Eng Mater 893:45–55. https://doi.org/10.1016/j.ijbiomac.2019.05.175
52. Azubuike CP, Mgboko MS, Ologunagba MO, Oseni BA, Madu SJ, Igwilo CI (2023) Preparation and characterization of corn cob cellulose acetate for potential industrial applications: Nigerian Journal of Pharmacy 57(2):709–718. https://doi. org/10.51412/psnnjp.2023.31
53. Qiao C, Ma X, Zhang J, Yao J (2017) Molecular interactions in gelatin/chitosan composite films. Food Chem 235:45–50. https://doi.org/10.1016/j.foodchem.2017.05.045
54. Li J, Shi X, Yang K, Guo L, Yang J, Lan Z, … Wang X (2024) Fabrication and characterization of carvacrol encapsulated gelatin/chitosan composite nanofiber membrane as active packaging material. Int J Biol Macromol 282:137114. https://doi.org/10.1016/j.ijbiomac.2024.137114
55. Cheah YJ, Yunus MHM, Fauzi MB, Tabata Y, Hiraoka Y, Phang SJ, … Yazid MD (2023) Gelatin–chitosan–cellulose nanocrystals as an acellular scaffold for wound healing application: fabrication, characterisation and cytocompatibility towards primary human skin cells. Cellulose 30(8):5071–5092. https://doi.org/10.1007/s10570-023-05212-w
56. Ahuja S., Patel A., Patel A., & Panda S. (2023) Antibacterial composite film prepared from microcrystalline cellulose-chitosan from libr solution with garlic extraction. International Journal of Biology, Pharmacy and Allied Sciences 12(1). https://doi.org/10.31032/IJBPAS/2023/12.1.6714